Structuring electrospun polycaprolactone nanofiber tissue scaffolds by femtosecond laser ablation

Hae woon Choi
Laboratory for Multiscale Materials Processing and Characterization, The Ohio State University, 1248 Arthur E. Adams Dr., Columbus, Ohio 43221

Jed K. Johnson and Jin Nam
Department of Materials Science and Engineering, The Ohio State University, 477 Watts Hall, 2041 College Road, Columbus, Ohio 43210

Dave F. Farson[a)]
Laboratory for Multiscale Materials Processing and Characterization, The Ohio State University, 1248 Arthur E. Adams Dr., Columbus, Ohio 43221

John Lannutti
Department of Materials Science and Engineering, The Ohio State University, 477 Watts Hall, 2041 College Road, Columbus, Ohio 43210

(Received 8 October 2006; accepted for publication 11 December 2006; published 18 October 2007)

Meshes of electrospun (ES) polycaprolactone (PCL) and polyethylene terephthalate nanofiber meshes were structured by ablation of linear grooves with a scanned femtosecond laser. Focus spot size, pulse energy, and scanning speed were varied to determine their affects on groove size and the characteristics of the electrospun fiber at the edges of these grooves. The femtosecond laser was seen to be an effective means for flexibly structuring the surface of ES PCL scaffolds. Femtosecond ablation resulted in much more uniformly ablated patterns compared to *Q*-switched nanosecond pulse laser ablation. Also, the width of the ablated grooves was well controlled by laser energy and focus spot size, although the grooves were significantly larger than the spot size. Also, some melting of fibers was observed at the edges of grooves. These affects were attributed to optical radiation from laser-induced plasma at higher pulse energies and melting of fibers at laser fluences lower than the ablation threshold. The ablation threshold for the PCL mesh was estimated to be significantly larger than that of bulk (solid) PCL, a result attributed to multiple scattering of the laser energy within the volume of the nanofiber mesh.

I. INTRODUCTION

Electrospun nanofiber mesh[1–4] is widely used as a tissue engineering scaffold to support cellular in-growth and proliferation for generation of biological tissues.[5–9] However, the randomly deposited structure of electrospun fiber does not allow for spatial control of cells necessary to produce complex organs *in vivo*. Cells typically grow only on the exterior surface of electrospun fiber following random seeding techniques.[2] Direct-write femtosecond laser ablation is a flexible, rapid structuring technique that has the potential to alter this via precise control of surface topography to produce specific microenvironments that can influence cellular growth patterns. This article describes the development of procedures for the ablation of linear and shaped grooves and cavity arrays that are to be used in subsequent tissue growth studies.

Polycaprolactone (PCL) and polyethylene terephthalate (PET) are commonly used in biomedical applications. PCL is a Food and Drug administration-approved biodegradable polyester. It has been used in biomedical applications in drug delivery devices, sutures and adhesion barriers, and is being investigated as a scaffold for tissue engineering. It has a relatively low melting temperature ($T_m \approx 60\ ^\circ\mathrm{C}$). PET is thermoplastic resin of the polyester family used biomedically under the trade name Dacron® as a vascular graft. It has higher transition temperatures than PCL (e.g., $T_m \approx 260\ ^\circ\mathrm{C}$). Specific polymers properties are listed in Table I; in this work, PET mainly provides a material comparison to PCL.

No prior reports have been found regarding laser ablation of electrospun (ES) fiber meshes but laser structuring of PCL films and membranes has been investigated. Thin films of biodegradable polymeric materials, poly(ε-caprolactone) have been micro-patterned using a Ti–sapphire femtosecond pulsed laser and an ArF excimer UV laser in ambient conditions.[10] Characterization of femtosecond laser ablated PCL by hydrolytic degradation tests showed that the laser irradiation had little affect. The permeability of ultrathin PCL produced by bi-axial stretching was enhanced by drilling using a femtosecond laser; the surface was rendered more hydrophilic (which typically enhances cellular adhesion) by excimer laser ablation texturing.[11]

The 775 nm, 150 fs ultrafast pulsed laser was considered promising for electrospun fiber structuring because ablation

[a)]Electronic mail: farson.4@osu.edu

TABLE I. Physical properties of PCL and PET.

Polymer	Melting temp. T_m (C)	Glass trans. Temp. T_g (C)	Thermal conductivity W/(m K)	Heat capacity kJ/(kg K)	Bulk density g/cm^3	ES mesh density g/cm^3	Solid density g/cm^4
PCL	58–63	−65∼−60	0.07*	1.3	1.14	0.24	1.2*
PET	130–137	75	0.13–0.15	1.3	1.3–1.4	⋯	⋯
*Starch blend							*PLC/PCL co-polymer

with the short, high irradiance pulses typically has minimal affects on the remaining material. The photon energy (1.6 eV) is too small for photochemical ablation,[12] but amplified femtosecond pulses can nonetheless be strongly absorbed and produce clean ablation in many materials. When energetic femtosecond laser pulses are incident on dielectric polymers, it is generally considered that nonlinear processes associated with the irradiance generate free electrons which are then responsible for increased absorption and consequent rapid heating, ionization, charge separation, and removal of the absorbing material.[12,13] Also, the thermal conduction length corresponding to the femtosecond laser pulse duration is generally small, so absorbed energy is not significantly diffused. It has been shown by a number of investigations that femtosecond pulsed laser ablation has fewer affects on the remaining polymer surface than nanosecond pulsed ablation at comparable wavelengths.[14–17]

Electrospun meshes have some similarities to photonic band gap crystals consisting of periodically spaced wavelength-sized structural units that have been widely studied in recent years. In the case of ES fiber meshes, fiber diameters are also on the order of the laser wavelength, but the sizes and locations are quite random. Thus, optical interactions likely have similarities to that encountered in characterization of human muscle tissue where radiation is highly scattered.[18,19]

This article describes microscale laser structuring of ES, PCL, and PET meshes. The fluence required for ablation as well as the affect of fluence and focus spot scanning speed on the dimensions of ablated grooves are determined. The fluences are compared to estimates of threshold fluence for ablation of the bulk materials. Key issues for the ablation development include preserving electrospun structure postablation, determining practical limits on lateral resolution and depth of ablated structures and establishing net ablation rates and process productivity. The structure of ES fiber remaining on the walls of femtosecond laser-ablated grooves in PCL and the regularity of machined grooves are compared to those of grooves produced by nanosecond laser ablation.

The fundamentals of femtosecond laser ablation have been summarized elsewhere.[13] For our purposes we can consider single pulse removal of a material with threshold ablation fluence F_{th} by a beam having a Gaussian radial fluence profile

$$F(r) = F_0 \exp(-2r^2/w_0^2), \tag{1}$$

where w_0 is Gaussian beam radius and F_0 is maximum (or peak) fluence, related to pulse energy E_p as

$$F_0 = 2E_p/\pi w_0^2. \tag{2}$$

If $F_0 > F_{\text{th}}$, the ablation threshold fluence, the diameter D of the area near the center of the beam from which material is removed is then

$$D^2 = 2w_0^2 \ln(F_0/F_{\text{th}}). \tag{3}$$

F_{th} can be found by curve fitting a semilogarithmic plot of D^2 measured for various F_0 and calculating the intercept at zero fluence.

II. EXPERIMENTAL APPARATUS AND PROCEDURE

Frequency doubled pulses from a mode-locked erbium-doped fiber laser intensified in a Ti:Al_2O_3 regenerative amplifier laser (CPA, Clark-MXR CPA2100) were used for this experiment. The maximum output power of the laser was $P_{\text{av}}=1.6$ W, the pulse duration was $T_p=150$ fs and the pulse repetition frequency was $f_p=2$ kHz. The output power was adjusted in two stages. The majority of the attenuation was at the first thin-film polarizing beam splitter, where only a couple percent of the optical power passes through to a 1/2 waveplate. The beam polarization was adjusted by rotation of this optical element, allowing the additional attenuation at the second polarizing beam splitter to be adjusted. The attenuated laser beam was delivered by a beam delivery mirror train through a mechanical shutter and focused on the material. A 25 mm focal length achromatic lens (NA=0.1), a 10x microscope objective (NA=0.25) and a 20x infinity-corrected microscope objective (also NA=0.25 with the 5 mm beam diameter) were the focusing optics used in the femtosecond laser experiments. To accurately measure processing power before experiments, a power meter was inserted after the focusing lens. Prior to performing the experiments, the M^2 beam quality parameter was measured with a charge coupled device camera and beam characterization software (SPIRICON). The beam quality was $M^2=1.2$ in the vertical Y direction and $M^2=1.3$ in the horizontal X direction. The calculated minimum focus spot diameter for the femtosecond laser with 0.1 NA lens is approximately 6.4 μm and that of the 0.25 NA objectives is 2.6 μm. Primarily for purposes of comparison, a Q-switched Nd:yttrium–aluminum–garnet (YAG) laser (TN-50, Spectra Physics) with $T_p=120$ ns at a pulse repetition frequency $f_p=10$ kHz, maximum average power $P_{\text{max}}=50$ W was also used. The beam diameter of this laser was $d_b=1.9$ mm and the quality factor was $M^2=15$. The numerical aperture when the focusing with the 25 mm achromatic lens was NA

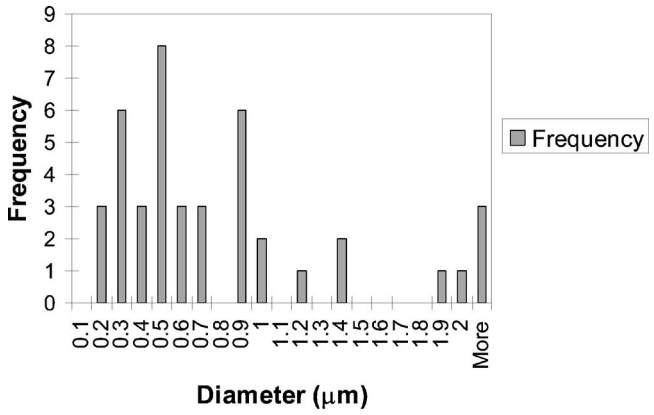

FIG. 1. Fiber diameter size distribution of ES-PCL meshes used in the experiments.

=0.037 and the estimated diffraction-limited spot diameter was d_0=271 μm. All ablation of linear grooves was done at a scanning speed of 20 mm/s.

Electrospun PCL was produced using a 12 wt% solution of PCL (M_w 65 000, Aldrich, St. Louis, MO) dissolved in acetone (Mallinckroff Chemicals, Phillipsburg, NJ) and pumped through a 20 gauge stainless steel blunt tip needle at a flow rate of 24 ml/h under an applied voltage of 24 kV. The tip-to-substrate distance was 16 cm. The fiber diameter ranged from 0.2 μm to more than 2 μm. The distribution of fiber sizes is given in Fig. 1. The ES PET was prepared using 12 wt% PET (M_w 18 000, Aldrich, St. Louis, MO) in a 50/50 solution of trifluoroacetic acid/dichloromethane. Electrospinning voltage was 22 kV, material flow rate was 18 ml/h and needle tip-substrate distance was 18 cm. The mechanical and electrical properties of PCL and PET (such as dielectric values and mechanical viscosity) affect the electrospinning process so the electrospun fiber diameter and fiber density are different. The density of the resulting mesh and other properties of the polymers are summarized in Table I.

To better understand the penetration of laser and plume energy into the ES PCL, the directional hemispherical transmittance of different thicknesses of electrospun and solid PCL were measured using an integrating sphere (IS236A, Thorlabs, Newton, NJ). The diameter of the samples used for these experiments was about 20 mm (compared to the unfocused beam diameter of 5 mm).

III. RESULTS

Linear grooves produced by scanning the focused femtosecond and nanosecond laser beams over the surface of electrospun PCL provided an initial comparison that established the benefits of the high intensity of pulses for ES nanofiber ablation. The power of both lasers and the Nd:YAG pulse frequency were varied in a series of experiments to determine feasible values for consistent ablation of microscale grooves. The average power of the femtosecond laser beam was varied between 5 and 200 mW while that of the *Q*-switched laser power was varied between 3 and 10 W; no ablation was found at less than 3 W. The distance between individual pulses on the mesh surface was 10 μm for

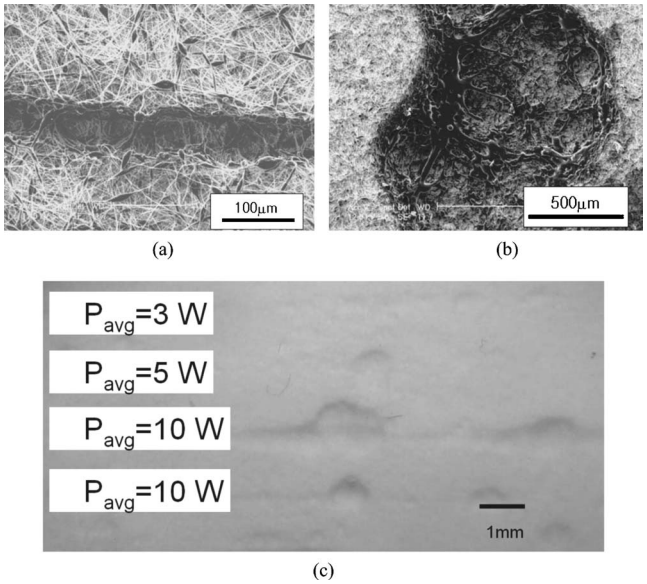

FIG. 2. SEM images of (a) femtosecond laser and (b) *Q*-switched laser grooves. The width of the femtosecond laser groove is approximately 35 μm. (c) *Q*-switched laser power was varied from 3 to 10 W, but no power that produced consistent ablation was determined.

the femtosecond laser and 2 μm for the *Q*-switched laser. Thus, the femtosecond laser pulses were not overlapped (spot diameter was only 6.4 μm) while the *Q*-switched laser pulse overlap was 99.3% of the larger focus spot diameter and higher pulse frequency. The higher overlap of Nd:YAG laser with high frequency was caused by the limitation of linear motion system scanning speed.

Scanning electron microscopy (SEM) images were used to measure the width of femtosecond-ablated grooves and to characterize the affects of groove ablation on the fibers remaining on the groove walls. It was evident from these initial results the femtosecond laser ablated a relatively uniform groove [Fig. 2(a)] with widths and depths that varied predictably with average power. Grooves produced by the femtosecond laser had minimal melting of the remaining fiber at the edges of the ablation area. In contrast, the width of the

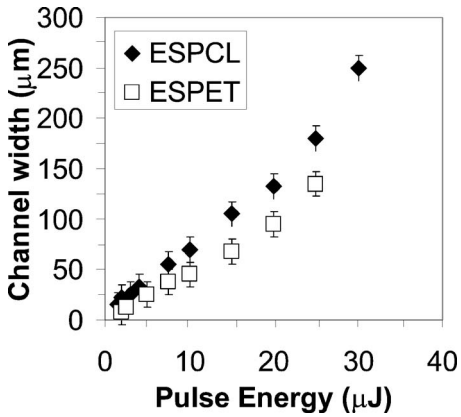

FIG. 3. Width of grooves machined in ES nanofiber meshes at various pulse energies using the 0.1 NA optic and speed of 20 mm/s. The groove width is generally much larger than the focus spot size of 6.4 μm. Error bars indicate error in estimating groove dimension.

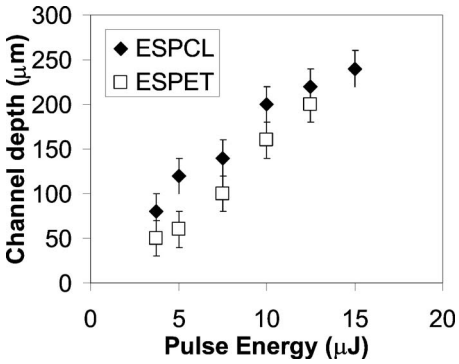

FIG. 4. Depth of grooves machined in ES nanofiber meshes at various pulse energies using the 0.1 NA optic and speed of 20 mm/s showing that PCL grooves were slightly deeper. Error bars indicate error is estimating groove dimension.

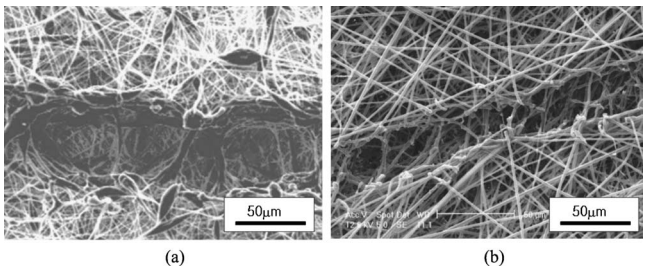

FIG. 5. Comparison of grooves in (a) PCL and (b) PET.

groove produced by the *Q*-switched laser varied unpredictably from practically 0 to almost 1 mm. As shown in Fig. 2(b), when it did ablate material, the *Q*-switched laser induced a high degree of fiber melting on the walls and bottom of the ablation area causing a high loss of the electrospun structure. At other times, in spite of the higher average power, practically no ablation was observed as shown in Fig. 2(c). The power was varied between 3 and 10 W and frequency changed between 5 and 50 kHz, but no significant improvement in consistency of grooves size was found.

The difference in laser machining results obtained with the *Q*-switched laser and femtosecond lasers is attributed to the affect of variations in the electrospun mesh density on the different ablation mechanisms for the two lasers. As mentioned in the Introduction, the high intensity femtosecond laser pulses input energy to the target material over a short time span and diffusion by thermal conduction is commensurately small. Thus, ionization and ablation tends to occur if the input fluence is over a distinct threshold magnitude. The energy input by lower intensity Nd:YAG laser pulses is converted to thermal energy in the material, which then melts and evaporates depending on the maximum temperature that is achieved. It seems likely that the unstable ablation behavior of the PCL nanofiber for Nd:YAG laser processing is related a transient increase of laser energy absorption associated with fiber melting.

To determine ablation properties electrospun mesh for femtosecond laser irradiation, grooves were created at different values of fluence by scanning with a focus spot for varying laser pulse energy. The experiments were conducted with 300-μm-thick meshes of PCL and PET on a glass substrate coated with 150 nm of transparent conductive film (ITO, indium tin oxide) to allow electrospinning. The 0.1 NA focus lens was used for the ablation and scanning speed was 20 mm/s. The groove width and depth were measured for both materials and their variation with pulse energy are plotted in Figs. 3 and 4. The widths of grooves formed are significantly wider than the focus spot size of 6.4 μm. It is also observed that the width and depth of grooves in PCL are somewhat larger than those formed in PET at the same laser fluence (examples of grooves in PCL and PET are shown in Fig. 5). The material removal rate for PCL mesh was calculated from the groove width, depth, and scanning speeds shown in Figs. 3 and 4 to be in the range of 0.1–1 mm^3/s. At the same femtosecond laser ablation fluence and scan speed, the volume removal rate of PET was from 1.5 to 3 times smaller. The difference in the material removal rate for the two polymers is at least partly attributed to differences in thermal properties.

Some melting of fibers at the edges of the machined grooves was produced by all of the tests described above. A

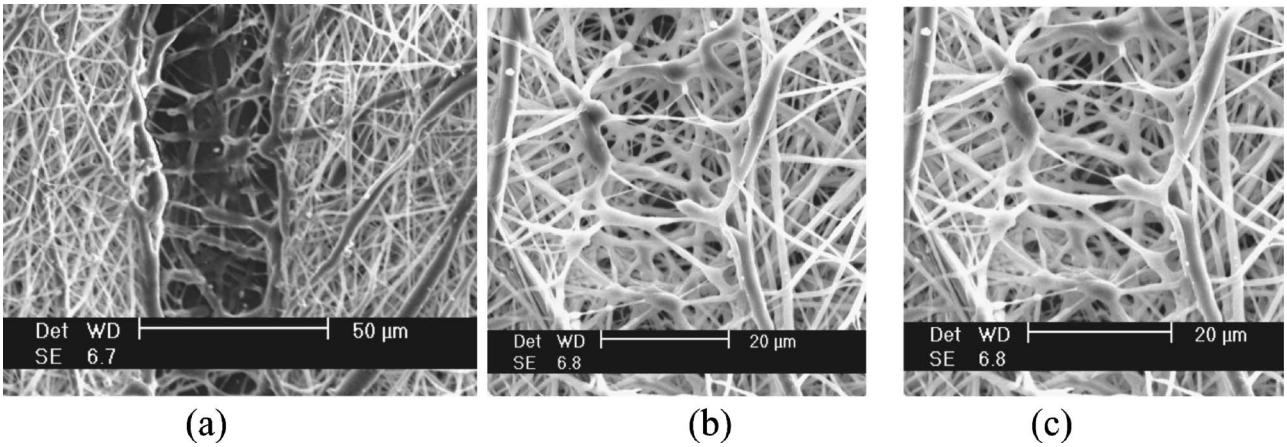

FIG. 6. Two grooves ablated in PCL nabofiber with the 0.1 NA optic at a speed of 20 mm/s and relatively low energy. (a) Pulse energy=1.5 μJ, fluence =9.3 J/cm^2; (b,c) pulse energy=0.75 μJ, fluence=4.6 J/cm^2.

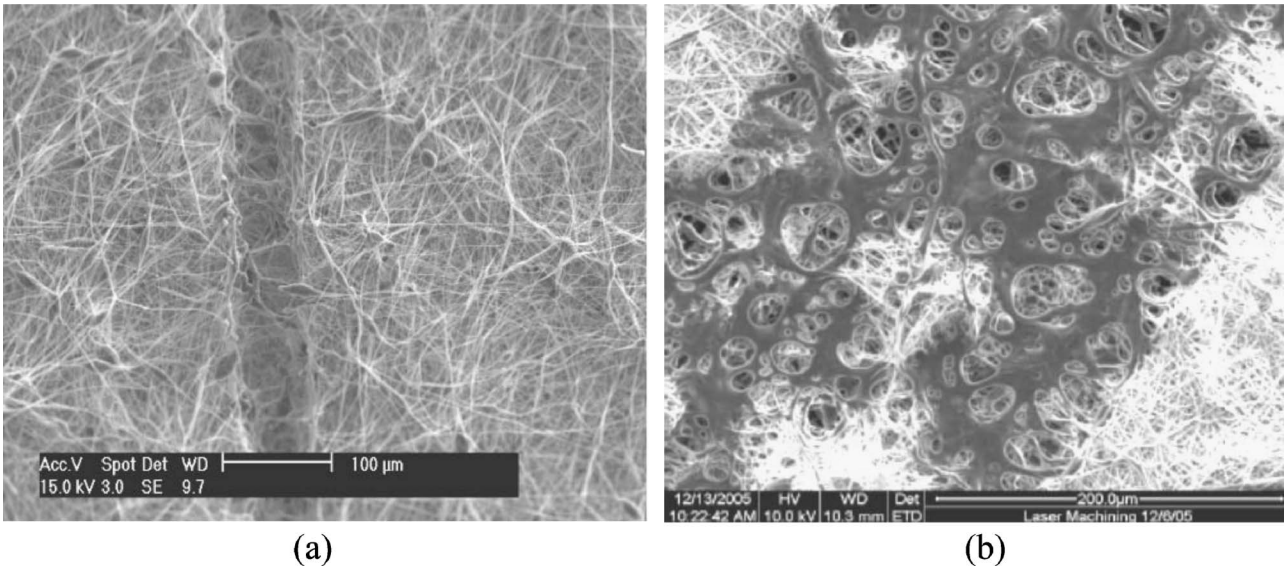

FIG. 7. (a) Focused and (b) defocused (multiple passes, right) scans showing that the lower fluence due to beam defocusing melted rather than ablated the mesh.

comparison of two grooves ablated in PCL at relatively low pulse energies is shown in Fig. 6. It is obvious that melting and fusing of groove wall fibers is increased with pulse energy and that some melting of the mesh fibers was evident even when the surface was not deeply structured by the ablation. Several instances of thinned fibers and fusion of overlapped fibers are seen in this example. At least some similar melting appears to be difficult to avoid with the femtosecond laser used in these tests. The large grooves produced at high pulse energy may be attributed to melting and ablation of fibers beyond the radius of laser beam impingement by optical radiation from the plasma formed by interaction of laser radiation with fibers. Such a plasma is easily visible at higher fluence conditions and is discussed below. Melting of fibers is also consistent with a conclusion that femtosecond pulses tended to melt rather than ablate the nanofibers when fluence dropped below the ablation threshold. This affect was explored further in experiments discussed below. In any case, cell growth tests currently being carried out indicate that the minimal melting incurred when structuring nanofiber meshes with femtosecond ablation has no detrimental affect on the functionality of the mesh as a tissue scaffold.

The affect of low-fluence femtosecond laser pulses was studied further by varying the distance from the 0.1 NA focus lens to the mesh surface during ablation. Such variations might be expected to occur in practice due to variations in mesh thickness and errors in setting lens position. For producing defocused patterns, the focal point location was set 150 μm above the mesh surface, the laser power was 6 mW, and multiple scans were spaced 30 μm apart. As with all tests, scan speed remained at 20 mm/s. The calculated spot diameter of the defocused beam was 30.7 μm, roughly five times that of the focused beam. The corresponding laser fluence was 0.3 J/cm^2. For comparison, grooves were ablated with a focused beam with power of 5 mW and fluence of 7.7 J/cm^2. As shown in Fig. 7, irradiation with the defocused laser beam produced mostly undesirable melting instead of ablation of the fibers. In contrast, the higher focused laser beam fluence in this test was larger than the single pass groove which was about 65 μm wide and minimal fiber melting was observed on the walls. However, observed widths of grooves ablated in nanofiber mesh are not consistent with the usual ablation analysis outlined in the Introduction where the ablation diameter varies logarithmically with the fluence. Based on the observation of a visible plasma during the femtosecond laser machining, it is believed that heating and melting of fibers by energy radiated from this plasma may contribute to wider-than-expected grooves. The formation of plasma above solid surfaces being machined by femtosecond laser radiation is a well-known limitation on the achievable precision of femtosecond laser ablation in air at ambient conditions and it has been well characterized by other researchers. The plasma expands rapidly shortly after the femtosecond laser pulse and is observed to persist for many tens of nanoseconds.[20,21] Given the relatively low thermal conductivity, heat capacity and melting temperature of the electrospun PCL, it is expected that radiation from the

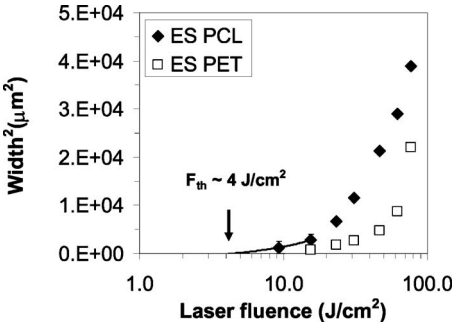

FIG. 8. Groove width squared of nanospun polymer vs fluence using the 0.1 NA optic showing nonlogarithmic behavior. The PCL ablation fluence threshold suggested by the lower end to the fluence curve is larger than the expected bulk value.

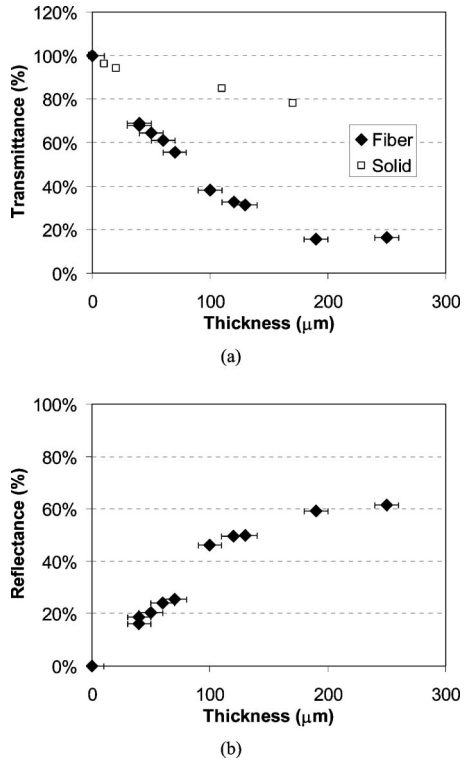

FIG. 9. (a) Hemispherical transmittance of ES PCL nanofiber mesh and solid PCL and (b) reflectance of nanofiber mesh for an unfocused femtosecond laser beam. Error bars indicate estimated ±10 μm accuracy in mesh thickness measurement.

plasma would be more effective for increasing the width and depth of grooves in it than in PET, in accordance with the experimental results.

The variation of the squared values of ablated groove width with fluence was analyzed to quantify the ablation threshold. This procedure is based on an assumption that the groove width and the ablation diameter of a single spot are equal. It has been shown in other thin film ablation work by the authors[22] that the width of lines ablated in thin film with femtosecond pulsed lasers still followed the expected logarithmic trend. As shown in Fig. 8, the ablation curves for electrospun PCL and PET mesh are nonlogarithmic. The slope of the curves is still decreasing at the lower two values plotted for PCL, so the threshold fluence value of 4 J/cm^2 was obtained by extrapolating these points find the x-axis intercept. In contrast, the expected ablation threshold value for bulk PCL[12] is less than 1 J/cm^2. The difference is explained when one considers the large surface area of the fibers within a volume defined by the laser focus spot diameter and extinction depth, as discussed below. A detailed analysis of the ablation properties of polymer nanofiber meshes for femtosecond laser pulses is the subject of current research by the authors.

To better understand the laser ablation characteristics of electrospun PCL, its absorption properties were measured. The results of directional hemispherical transmittance tests of electrospun and solid PCL are plotted in Fig. 9. Since it is not a very highly scattering material when solid, the absorption coefficient for the solid PCL was approximated directly from this curve as 0.0013 μm^{-1}, corresponding to an absorption length of about 770 μm. The decrease of mesh transmittance with thickness is well approximated by an exponential function and the extinction coefficient is about 0.0085 μm^{-1}, corresponding to an extinction depth of approximately 120 μm. Thus, the fiber mesh extinction coefficient is much larger than the solid material absorption coefficient, in spite of the fact that the measured mesh density was ρ_m =0.24 g/cm^3, about 20% that of the solid material density. If extinction were primarily due to absorption, the extinction coefficient for low-density nanofiber mesh would be expected to be less than that of the solid material. Thus, the large mesh extinction confirms that scattering rather than absorption is a dominant factor in the attenuation of laser radiation through the mesh. The groove depths produced by laser ablation were on the order of the measured fiber mesh extinction length of 120 μm, as would be expected. The groove widths are also of the same order as the extinction

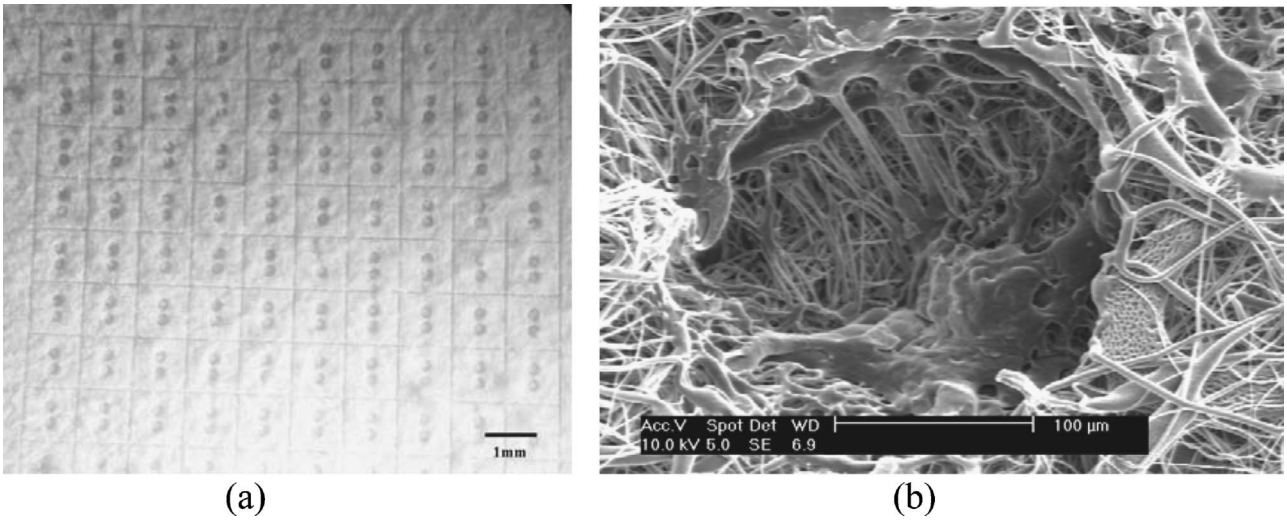

FIG. 10. (a) Matrix of microscale structures ablated in PCL nanofiber mesh and (b) magnified view of a laser-machined cavity in PCL nanofiber mesh (right) begin used in a cell culture test.

length. This is consistent with a hypothesis that radiated plume light is influential in determining the size of ablated features, since the lateral penetration of radiation would also be expected to be limited by scattering. However, such a conclusion needs to be confirmed by measurements of extinction length is a direction parallel to the mesh surface since the mesh appears to be rather nonisotropic in the SEM images.

It is also interesting to revisit the ablation threshold estimated for the nanofiber mesh in view of the measured characteristic extinction depth of laser light. A typical fiber spacing of 2 μm is estimated from the fiber diameter distribution shown in Fig. 1 and the fractional density of nanofiber mesh as compared to solid material. Given that the incoming light is scattered multiple times within the extinction length of 120 nm, the fiber mesh before being absorbed, it is very plausible that the material surface area illuminated by a femtosecond laser pulse is much larger than the focus spot area and thus, the ablation threshold determined for fiber mesh is corresponding larger for the fiber mesh than for solid material. A detailed analysis of ablation of nanofiber mesh by femtosecond laser pulses is currently being carried out by the authors.

After the study described above, shaped grooves were ablated in the surface of electrospun PCL in preparation for specific tissue growth studies. As shown in Fig. 10(a), laser ablation was used to form a 1 mm grid pattern with a microstructured cavity at the center of each grid cell. Ablation parameters were the same as those used to ablate the straight groove in Fig. 6. In Fig. 10(b), a magnified view of a cavity being used for a cell culture test and a cluster of cells can be observed with growth constrained to the bottom of the cavity.

IV. CONCLUSIONS

The femtosecond laser was effectively used for ablation of meshes of electrospun PCL and PET polymers. Laser ablation resulted in uniform ablation grooves with width and depth controlled by femtosecond laser pulse fluence at constant scanning speed. It was observed that the maximum width of the grooves was generally much larger than the laser focus spot size. While some melting of fibers was observed on the edges of grooves ablated by the femtosecond lasers, the melting was minimal compared to that observed for grooves ablated with a Q-switched laser. The large widths of ablated grooves were attributed to material removal by optical radiation from laser-induced plasma. The extinction coefficient of PCL nanofiber meshes was measured and found to be high relative to the absorption coefficient of the bulk material. This indicated that scattering was the dominant mechanism for extinction, a fact that was used to explain the observation that the estimated ablation thresholds of the fiber materials were somewhat larger than the bulk materials.

[1] P. K. Baumgarten, "Electrostatic spinning of acrylic microfibres," J. Colloid Interface Sci. **36**, 71–79 (1971).
[2] J. Lannutti, D. Reneker, T. Ma, D. Tomasko, and D. F. Farson, Mater. Sci. Eng., C **27**, 504–509 (2007).
[3] D. H. Reneker and I. Chun, "Nanometre diameter fibres of polymer, produced by elcetrospinning," Nanotechnology **7**, 216–223 (1996).
[4] K. H. Lee, H. Y. Kim, M. S. Khil, Y. M. Ra, and D. R. Lee, "Characterization of nanostructured poly(ε-caprolactone) nonwoven mats via electrospinning," Polymer **44**, 1287–1294 (2003).
[5] S. Kidoaki, I. K. Kwon, and T. Matsuda, "Mesoscopic spatial designs of nano- and microfiber meshes for tissue-engineering matrix and scaffold based on newly devised multilayering and mixing electrospinning techniques," Biomaterials **26**, 37–46 (2005).
[6] W. J. Li, C. T. Laurencin, E. J. Caterson, R. S. Tuan, and F. K. Ko, "Electrospun nanofibrous structure: A novel scaffold for tissue engineering," J. Biomed. Mater. Res. **60**, 613–621 (2002).
[7] H. Yoshimoto, Y. M. Shin, H. Terai, and J. P. Vacanti, "A biodegradable nanofiber scaffold by electrospinning and its potential for bone tissue engineering," Biomaterials **24**, 2077–2082 (2003).
[8] C. Y. Xu, R. Inai, M. Kotaki, and S. Ramakrishna, "Aligned biodegradable nanotibrous structure: A potential scaffold for blood vessel engineering," Biomaterials **25**, 877–886 (2004).
[9] B. M. Min, G. Lee, S. H. Kim, Y. S. Nam, T. S. Lee, and W. H. Park, "Electrospinning of silk fibroin nanofibers and its effect on the adhesion and spreading of normal human keratinocytes and fibroblasts in vitro," Biomaterials **25**, 1289–1297 (2004).
[10] C. A. Aguilar, Y. Lu, S. Mao, and S. C. Chen, "Direct micro-patterning of biodegradable polymers using ultraviolet and femtosecond lasers," Biomaterials **26**, 7642–7649 (2005).
[11] K. S. Tiaw, S. W. Goh, M. Hong, Z. Wang, B. Lan, and S. H. Teoh, "Laser surface modification of poly(epsilon-caprolactone) (PCL) membrane for tissue engineering applications," Biomaterials **26**, 763–769 (2005).
[12] T. Lippert, "Interaction of photons with polymers: From surface modification to ablation," Plasma Processes Polym. **2**, 525–546 (2005).
[13] J. Kruger and W. Kautek, "Ultrashort pulse laser interaction with dielectrics and polymers," Adv. Polym. Sci. **168**, 247–289 (2004).
[14] S. Küper and M. Stuke, "Femtosecond UV excimer laser ablation," Appl. Phys. B **44**, 199–204 (1987).
[15] S. Küper and M. Stuke, "Ablation of polytetrafluoroethylene (Teflon) with femtosecond UV excimer laser pulses," Appl. Phys. Lett. **54**, 4–6 (1989).
[16] M. Womack, M. Vendan, and P. Molian, "Femtosecon pulsed laser ablation and deposition of thin films of polytetrafluoroethylene," Appl. Surf. Sci. **221**, 99–109 (2004).
[17] S. Baudach, J. Bonse, J. Krüger, and W. Kautek, "Ultrashort pulse laser ablation of polycarbonate and polymethylmethacrylate," Appl. Surf. Sci. **154**, 555–560 (2000).
[18] H. Dehghani, B. Brooksby, K. Vishwanath, B. W. Pogue, and K. D. Paulsen, "The effects of internal refractive index variation in near-infrared optical tomography: A finite element modelling approach," Phys. Med. Biol. **48**, 2713–2727 (2003).
[19] P. C. Waterman, "Scattering, absorption, and extinction by thin fibers," J. Opt. Soc. Am. A **22**, 2430–2441 (2005).
[20] B. Salle, O. Gobert, P. Meynadier, M. Perdrix, G. Petite, and A. Semerok, "Femtosecond and picosecond laser microablation: Ablation efficiency and laser microplasma expansion," Appl. Phys. A **69**, S381–S383 (1999).
[21] S. M. Klimentov, T. V. Kononenko, P. A. Pivovarov, S. V. Garnov, V. I. Konov, A. M. Prokhorov, D. Breitling, and F. Dausinger, "The role of plasma in ablation of materials by ultrashort laser pulses," Quantum Electron. **31**, 378–382 (2001).
[22] H. W. Choi, D. F. Farson, J. Bovatsek, A. Arai, and D. Ashkenasi, "Direct-write patterning of ITO film by high pulse repetition rate femtosecond laser ablation," Appl. Opt. **46**, 5792–5799 (2007).